Princeton Plasma Physics Laboratory

PPPL-4165

PPPL-4165

Spherical Torus Design Point Studies

C. Neumeyer, Y-K. Peng,
C. Kessel, and P. Rutherford

June 2006

Prepared for the U.S. Department of Energy under Contract DE-AC02-76CH03073.

Princeton Plasma Physics Laboratory
Report Disclaimers

Full Legal Disclaimer

Trademark Disclaimer

PPPL Report Availability

Princeton Plasma Physics Laboratory

This report is posted on the U.S. Department of Energy's Princeton Plasma Physics Laboratory Publications and Reports web site in Fiscal Year 2006.

The home page for PPPL Reports and Publications is:

http://www.pppl.gov/pub_report/

Office of Scientific and Technical Information (OSTI):

Available electronically at: http://www.osti.gov/bridge.

Available for a processing fee to U.S. Department of Energy and its contractors, in paper from:

U.S. Department of Energy
Office of Scientific and Technical Information
P.O. Box 62
Oak Ridge, TN 37831-0062

Telephone: (865) 576-8401

Fax: (865) 576-5728

E-mail: reports@adonis.osti.gov

Spherical torus design point studies

C Neumeyer[1], Y-K M Peng[2,3] , C Kessel[1], and P Rutherford[1]

[1]Princeton Plasma Physics Laboratory, PO Box 451, Princeton, New Jersey, 08543, USA
[2]Oak Ridge National Laboratory-UT Batelle, PO Box 2009, Oak Ridge, TN 37831, USA
[3]On assignment at Princeton Plasma Physics Laboratory

E-mail: neumeyer@pppl.gov

Abstract. The development path for the Spherical Torus (ST) is envisioned to lead to a Component Test Facility (CTF) (Peng *et al* 2005 *Plasma Phys. Control. Fusion* **47** B263) and possibly to an ST-based DEMO. The progression from present day ST experiments such as the National Spherical Torus Experiment (NSTX) (Synakowski *et al* 2004 *Nucl. Fusion* **43** 1648) and the Meg-Ampere Spherical Tokamak (MAST) (Lloyd *et al* 2004 *Plasma Phys. Control.* Fusion **46** B477) through intermediate devices to the CTF and DEMO needs to be guided by strategic consideration of scientific and technological steps which can be taken along the way with an appropriate balance of advancement versus risk. Parametric studies are an essential part of this process, and must be performed using methods which are efficient but comprehensive enough to capture key physics and engineering details using a common method to evaluate design point options over a wide range. This article describes the "systems code" methodology developed by the authors starting from prior work by others (Jardin *et al* 2003, *Fusion Sci. Tech.* **43**) and then improved in terms of physics and engineering algorithms and mathematical approach. In addition, some benchmarking and design point results are presented.

1. Introduction....4
2. Organization and Logic....4
3. Definitions....4
4. Physics Algorithms....5
4.1 Elongation (κ) Aspect Ratio Dependence....5
4.2 MHD Safety Factor....6
4.3 MHD Safety Factor Aspect Ratio Dependence....7
4.4 Plasma Current....8
4.5 Density and Temperature Profiles....8
4.6 Beta Limits and Aspect Ratio Dependence....9
4.7 Bootstrap Current Fraction....10
4.8 Neutral Beam Injection (NBI) Energy....11
4.9 Current Drive....11
4.10 Density....12
4.11 Separate Ion and Electron Power Balance....13
4.11.1 Neutral Beam Heating of Ions and Electrons....14
4.11.2 Alpha Heating of Ions and Electrons....15
4.11.3 Ion-Electron Equilibrium....16
4.12 Temperature....16
4.13 Radiation....17
4.14 Alpha Power....17
4.14.1 Thermal Ion Fusion....17
4.14.2 Two-Component Beam-Target Fusion....17
4.14.3 Integration of Fusion Power Over Plasma Volume....19
4.15 Plasma Stored Energy....20
4.16 Energy Confinement Time....20
4.17 Confinement Enhancement Factor....22
4.18 Fast Ion Effects....22
4.18.1 Alpha contributions....22
4.18.2 Beam ion contributions....23
5. Engineering Algorithms....23
5.1 Engineering Algorithms for Pulsed Copper Machine....24
5.1.1 Waveform Assumptions....24
5.1.2 Conductor Heating....24
5.1.3 Mechanical Stress in Coils....26
5.1.4 Solenoid Flux Requirement....28
5.2 Engineering Algorithms for Reactor....29
5.2.1 First Wall and Toroidal Field Inner Leg....29
5.2.2 Toroidal Field Outer Leg Return....30
5.2.3 Determination of Toroidal Field, Current, Input Power....31
5.2.4 Poloidal Field Requirements....32
5.2.5 Divertor and First Wall Heat Loads....32
5.2.6 Neutron Wall Loading....33
5.2.7 Blanket Coverage....33
5.2.9 Gross Thermal Power....38

5.2.10 Electric Power Consumption or Production 39
5.2.11 Tritium Consumption 39
6. Solver Operations 40
7. Sample results 42

1. Introduction

In preliminary studies of the design space available for toroidal fusion devices, it is beneficial to carry out parametric studies using "systems codes" which provide insight into design trade-offs and range of performance. This approach has become increasing more common as the physics, engineering, and technology basis for fusion has evolved during the past decades, particularly for the tokamak and the spherical torus (ST) configurations, where the interactions among these design topics are complex and nonlinear in nature.

Relatively robust numerical approaches to optimize an object function (i.e. figure of merit, such as modeled cost or size of the device), under the constraints of various design rules and limitations, have been developed and used in recent design assessments. In this paper, we will describe the content and application of such a systems code utilizing Microsoft EXCEL and its non-linear "solver". We will describe the physics, engineering, and technology assumptions incorporated in the code as simplified models that span a range of the plasma aspect ratio A (=R0/a) of interest to tokamaks and STs. We will show examples of applications of this code to model experiments today and project to future designs of interest to the fusion program.

2. Organization and Logic

Physics and engineering algorithms are processed using Microsoft EXCEL and its non-linear "solver" (Frontline Systems, Inc. http://www.solver.com/xlscompare.htm). The physics approach relies on a variety of well established formulae consisting of one dimensional functions as well as two dimensional functions numerically integrated over the plasma cross section. Thus the characterization of the approach as "1-1/2d". Key physics parameters which relate to stability are constrained by limits determined by algorithms derived from MHD equilibrium studies by Menard[5], Wong[6] and Lin-Liu[7] over a range of aspect ratio A. While the physics algorithms are valid over the full range of devices, the engineering algorithms depend on the specific details of machine construction (e.g. magnets) as well as the time duration of the operation (e.g. pulsed or steady state). Therefore several variants of the code are needed to address different types of machines.

3. Definitions

The plasma cross section (95% flux surface, containing 95% of the plasma poloidal magnetic flux) is shown in figure 1 and described by the following equations

$$R(\theta) = R_0 + a * \cos(\theta + \delta * \sin(\theta))$$

$$Z(\theta) = \kappa * a * \sin(\theta)$$

where:

R_0 = major radius (m)
a = minor radius (m)
A = aspect ratio = R_0 /a
ε = inverse aspect ratio = $1/A$
κ = elongation
δ = triangularity
θ = poloidal angle

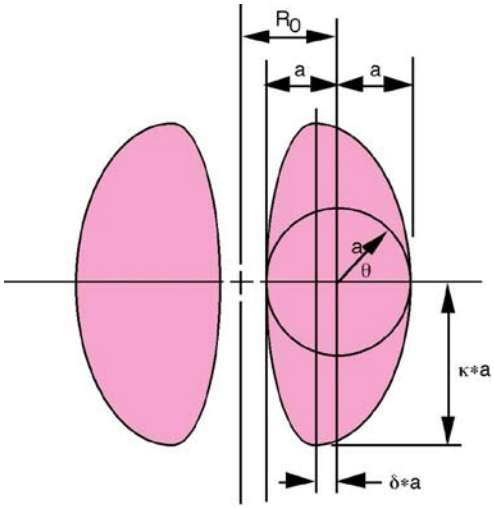

Figure 1. Plasma cross section

In determining the size of the vacuum vessel it is necessary to consider the entire plasma volume. Therefore we define A_{100} and a_{100} geometric quantities related to the 100% flux surfaces and use these to determine the vacuum vessel geometry for engineering purposes. The relationship between the 95% and 100% quantities was derived based on a pair of equilibria generated at A=1.5 and A=2.5 which bracket the aspect ratio range being considered in the subject study with typical values of triangularity and elongation. The following linear relationship was derived:

$$A_{100} = A(m * a + b)$$

where:

a = 0.017
b = 0.932

4. Physics Algorithms

The physics equations describe fundamental relationships between plasma variables but do not have a unique solution and cannot be solved directly as a group since the number of unknowns exceeds the number of equations. To obtain a solution for a particular plasma state the equations are divided into linked subsets which can be solved given a set of inputs. Then the solver is used to find a solution which satisfies linkages between the subsets as well as an optimization criteria. This section presents the physics equations in the order of calculation sequence.

4.1 Elongation (κ) Aspect Ratio Dependence

According to Menard the maximum κ as a function of inverse aspect ratio ε is as follows:

$$\kappa_{\max} = 1.46155 + 4.13281\varepsilon - 2.57812\varepsilon^2 + 1.41016\varepsilon^3$$

Similarly, according to Wong as a function of aspect ratio:

$$\kappa_{\max} = 1.082 + \frac{2.747}{A}$$

A comparison of these results is given in figure 2.

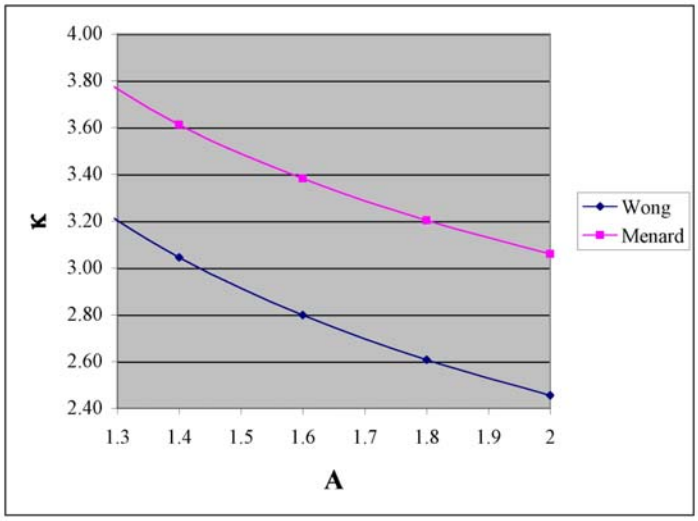

Figure 2. Maximum elongation κ vs. aspect ratio A

The work described herein typically uses the average of the Wong and Menard formulations.

4.2 MHD Safety Factor

The MHD safety factor, number of toroidal rotations per poloidal rotation of a field line on the 95% flux surface, is expressed in two forms, namely q_{cyl} and q_{MHD}, which are defined as follows:

$$q_{cyl} = \frac{5a^2 B_T}{I_p R_0}\left[\frac{1+\kappa^2}{2}\right]$$

$$q_{MHD} = \frac{5a^2 B_T}{I_p R_0}\left[\frac{1+\kappa^2\left(1+2\delta^2-1.2\delta^3\right)}{2}\right]\left[\frac{1.17-0.65\varepsilon}{\left(1-\varepsilon^2\right)^2}\right]$$

where:

B_T = vacuum toroidal field at R_0 (T)
I_p = plasma current (MA)

The calculations described herein rely primarily on q_{cyl} and report q_{MHD} as an output, for information only.

4.3 MHD Safety Factor Aspect Ratio Dependence

According to Menard the minimum safety factor as a function of aspect ratio is:

$$q_{cyl\_\min} = 12.259 - 13.58A + 6.4286A^2 - 1.0417A^3$$

Note: Menard prescribed $\beta_{Tmax}(\varepsilon)$, $\beta_{Nmax}(\varepsilon)$, and $\kappa_{max}(\varepsilon)$. The writers extracted q_{cyl} min(A) according to:

$$\beta_{P\max} = \frac{25}{\beta_{T\max}}\left[\frac{1+\kappa^2}{2}\right]\beta_{N\max}{}^2$$

and:

$$q_{cyl\min} = \sqrt{\frac{\beta_{P\max}}{\beta_{T\max}}\left[\frac{1+\kappa^2}{2A^2}\right]}$$

According to Wong the minimum safety factor as a function of aspect ratio is:

$$q_{cyl\_\min} = 1.21 + 1.3A - 0.25A^2$$

A comparison of these results is given in figure 3.

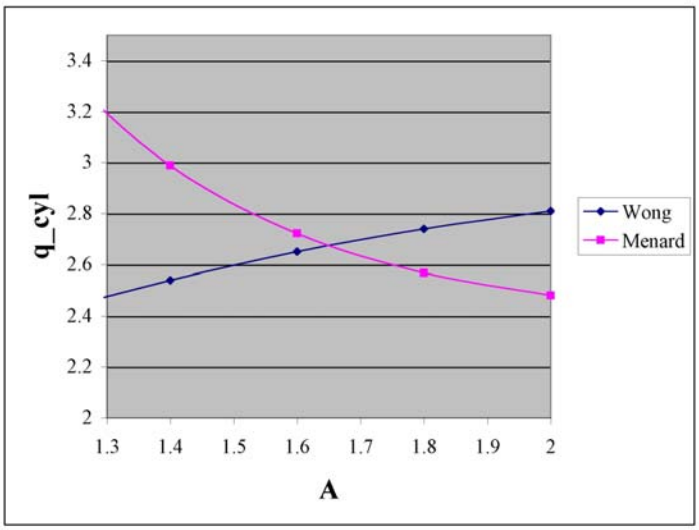

Figure 3. Safety factor vs. aspect ratio A

The work described herein typically uses the Wong formulation for q_{cyl_min}.

4.4 Plasma Current

With R_0,a,κ, and q_{cyl} determined the plasma current (in MA) is calculated according to:

$$I_p = \frac{5\times10^{-6}a^2B_T}{q_{cyl}R_0}\left[\frac{1+\kappa^2}{2}\right] = \frac{5\times10^{-6}R_0\varepsilon^2B_T}{q_{cyl}}\left[\frac{1+\kappa^2}{2}\right] = \frac{\pi R_0\varepsilon^2B_T\left(1+\kappa^2\right)}{10^6 q_{cyl}\mu_0}$$

$$I_p = \frac{\pi R_0\varepsilon^2B_T\left(1+\kappa^2\right)}{10^6 q_{cyl}\mu_0}$$

4.5 Density and Temperature Profiles

In prior work, spatial distribution of temperature and density across the plasma cross section were assumed to be parabolic to a power according to:

$$T(r) = T_0\left[1-\left(\frac{r}{a}\right)^2\right]^{\alpha_T}$$

$$n(r) = n_0\left[1-\left(\frac{r}{a}\right)^2\right]^{\alpha_N}$$

where:

r = variable in minor radius
a = minor radius of plasma = R_0/A
T_0,n_0 = central peak temperature and density at r=0
α_T, α_N = shape exponents on temperature and density

These forms are convenient because related integrals can be readily solved in analytic form. However in our recent work we include additional terms which allow a more realistic profiles over which we can integrate numerically. Thus we represent temperature, density, and heating power using the following form:

$$x(r) = x_0\left[1-(1-\beta-\delta)*\left(\frac{r}{a}\right)^2-\beta*\left(\frac{r}{a}\right)^4-\delta*\left(\frac{r}{a}\right)^8\right]^{\alpha}$$

We choose the coefficients α, β, and δ based on fits to experimental results on NSTX. We perform numeric integrations over the profile subdivided into 100 steps in r/a, and also compute peak to average ratios numerically.

4.6 Beta Limits and Aspect Ratio Dependence

According to Menard an appropriate limit on β_N is as follows:

$$\beta_{Nmax}(\varepsilon) = \frac{6.96436 - 14.043\varepsilon + 45.5\varepsilon^2 - 31.3086\ \varepsilon^3}{100}$$

According to Wong the β_N limit depends on A, κ, and pressure peaking factor. The peaking factor is as follows:

$$Peakfactor = \left(\int_0^1 \left[1 - x^2\right]^{\alpha_T} \left[1 - x^2\right]^{\alpha_N} dx \right)^{-1}$$

where x=r/a. Then the β_N limit is:

$$\beta_{Nmax}(A) = \frac{\left(3.09 + \frac{3.35}{A} + \frac{3.87}{A^{0.5}}\right)\left(\frac{\kappa}{3}\right)^{0.5}}{100 * Peakfactor^{0.5}}$$

According to Lin-Liu the β_N limit is as follows:

$$\beta_{Nmax}(A) = \frac{-0.7748 + 1.2869\kappa - 0.2921\ \kappa^2 + 0.0197\kappa^3}{\tanh((1.8524 + 0.2319\kappa)/A^{0.6163}))A^{0.5523}/10}$$

It is noted that the above includes a dependency on elongation. A comparison of these results is given in figure 4, including the Lin-Liu equation using the kappa values from Menard and Wong.

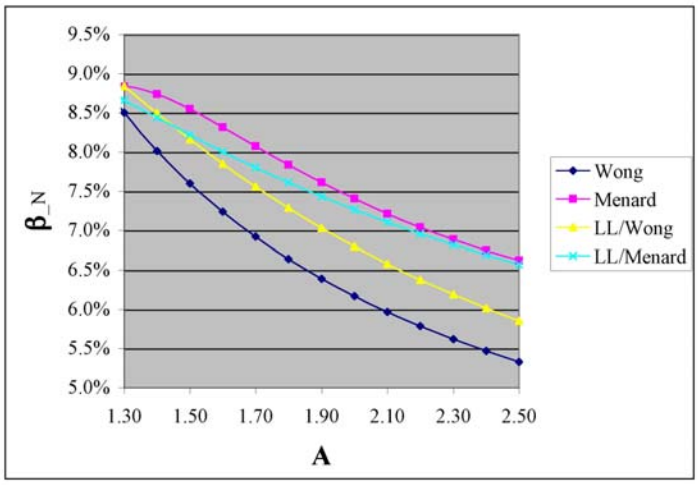

Figure 4. Max. β_N vs. A

The work described herein relies primarily on the Lin-Liu formula.

The solver arrives at a value for total pressure $\beta_{N\text{-}Total}$ which must be $\leq \beta_{Nmax}$. This total includes the partial pressures due to thermal ions and electrons as well as energetic ions consisting of alpha particles and neutral beam injected ions. The total pressure resulting from the thermal ions and electrons is referred to simply as β_N. Therefore:

$$\beta_N = \beta_{N\_Thermal\_i} + \beta_{N\_Thermal\_e}$$

$$\beta_{N\_Total} = \beta_N + \beta_{N\_\alpha} + \beta_{N\_nbi} \leq \beta_{N\_Max}$$

With β_N and other variables previously determined, β_T can β_P can be calculated based on their definitions as follows:

$$\beta_T = \frac{I_P A \beta_N}{R_0 B_T} = \frac{I_P \beta_N}{R_0 \varepsilon B_T}$$

$$\beta_P = \frac{2\beta_T q_{cyl}^2 A^2}{\left(1+\kappa^2\right)}$$

Finally, the volume averaged pressure is:

$$< P >= \frac{\beta_N I_P B_T}{2\mu_0 a}$$

4.7 Bootstrap Current Fraction

Bootstrap current fraction f_{BS} is dependant on β_P and aspect ratio as follows:

$$f_{BS} = \frac{X\beta_P}{\sqrt{A}} = X\beta_P\sqrt{\varepsilon}$$

where X is a function containing terms related to shape and profile. In the work described herein we apply a curve fit function $X = k_{BS}(A)*Peakfactor^{0.25}$ which results in $f_{BS} = 0.9$ for the Wong case and $f_{BS} = 0.99$ for the Menard case since these were the applicable bootstrap fractions for the MHD stability analysis performed. Therefore f_{BS} is calculated as follows:

$$f_{BS} = k_{BS} * Peakfactor^{0.25} * \beta_P\sqrt{\varepsilon}$$

where for Menard:

$$k_{BS}(A) = 0.344 + 0.195 * A$$

and for Wong:

$$k_{BS}(A) = 0.6783 + 0.0446/A$$

A comparison of these results is given in figure 5.

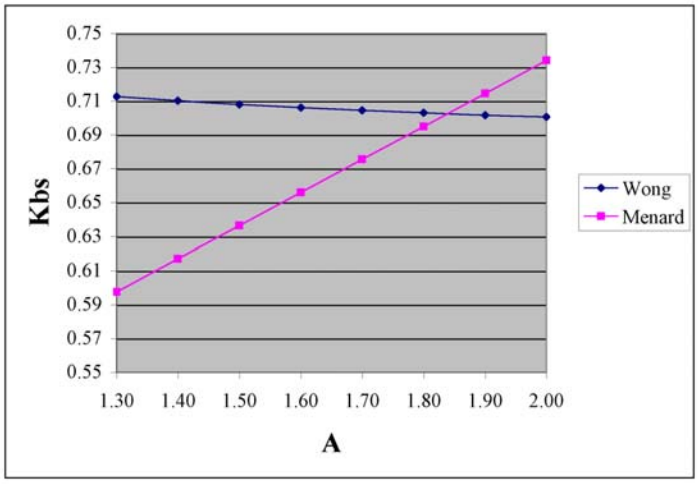

Figure 5. Bootstrap Coefficient vs. A

4.8 Neutral Beam Injection (NBI) Energy

Beam power deposition calculations were performed for cases which bracket the size, aspect ratio and density of interest. Based on this information it was determined that the required beam energy to give parabolic-like deposition profiles with tangential injection at R_0 can be approximated by:

$$E_b = 100\langle n_{e-20}\rangle L_b$$

where the beam path length L_b is the beam distance to the plasma axis:

$$L_b = \left[(R_0 + a)^2 - R_0^{\,2}\right]^{1/2}$$

4.9 Current Drive

The current drive efficiency parameter is defined as follows:

$$\gamma_{CD} = \frac{n_{20} I_{CD} R_0}{P_{CD}}$$

where:

γ_{CDMAX} = maximum efficiency in units 10^{20}Ampere/Watt-m^2
n_{20} = electron density in units 10^{20}Ampere/Watt-m^2
I_{CD} = current to be driven in MA
P_{CD} = current drive power in MW

Data for current drive efficiency from Start and Cordey [8] was curve fit with the following result:

$$\gamma_{CD} = E_{nbi}^{\,0.5327}(-8.471\text{x}10^{-4} + 1.852\text{x}10^{-3} T_{avg} - 5.307\text{x}10^{-5} T_{avg}^2)$$

where:

E_{nbi} = neutral beam energy
T_{avg} = average electron temperature (simple average, not density weighted)

The current to be driven is $I_p*(1-f_{BS})$, and the current drive power (MW) requirement is therefore:

$$P_{CD} = \frac{n_e R_0 I_p (1 - f_{BS})}{10^{20} \gamma_{CD}}$$

where n_e is the electron density. Neutral beam injection (NBI) is assumed to provide the auxiliary heating power (P_{aux}) and current drive power. The solver is constrained in such a way that $\gamma_{CD} \leq \gamma_{CDmax}$ and $P_{CD} \leq P_{aux}$.

4.10 Density

Line average electron density is related to the fraction of Greenwald Limit [9] f_{GW} as follows:

$$\overline{n_e} = \frac{f_{GW} I_p * 10^{20}}{\pi a^2} = \frac{f_{GW} I_p * 10^{20}}{\pi R_0^2 \varepsilon^2}$$

Electron density (volume average) is:

$$< n_e >= \frac{\overline{n_e}}{\left(1 + \frac{\alpha_N}{2}\right)}$$

Helium ash density (volume average) is calculated as follows. For power balance, total power into the plasma equals power out :

$$P_{Tot} = P_\alpha + P_{aux} - P_{rad} = P_\alpha + \frac{P_{fusion}}{Q} - P_{rad} = P_\alpha \left(1 + \frac{5}{Q} - f_{rad}\right) = \frac{W}{\tau_E}$$

where:

P_α = power in α particles
P_{aux} = auxiliary heating power
P_{rad} = radiated power
P_{fusion} = total fusion power
Q = fusion power gain
f_{rad} = radiation fraction = P_{rad}/P_α
W = stored energy
τ_E = energy confinement time

For α particle balance, the rate of α production from fusion reactions must equal the rate of α particle loss:

$$\frac{P_\alpha}{W_\alpha} = \frac{n_{He}}{\tau_p^*}$$

where:

W_α = energy per α particle, equal to 3.52MeV*1.6x10^{-13}Joule/MeV=5.63x10^{-13}Joule
τ^*_p= α particle confinement time after adjusting for recycling

The stored energy is related to the pressure as follows:

$$W = \frac{3}{2} < P >= \frac{3}{2}\frac{\beta_N I_P B_T}{2\mu_0 a}$$

Rearranging the prior three equations yields the following for helium ash density:

$$n_{He} = \frac{3}{2}\left[\frac{\beta_N I_P B_T}{2\mu_0 a}\right]\left[\frac{\tau_P^*}{\tau_E}\right]\left[5.63\times 10^{-13}\left(1+\frac{5}{Q}-frad\right)\right]^{-1}$$

The ratio τ^*_p/τ_E is an input variable typically assumed equal to 5.0. For impurities, Be is typically assumed the dominant species (Z_{imp}=4) at a concentration f_{imp} = 6%. For charge neutrality, with Z=2 for He:

$$n_e = n_{DT} + 2n_{He} + Z_{imp} n_{imp}$$

The impurity density (volume average) is:

$$n_{imp} = n_e * f_{imp}$$

The density (volume average) of H species (D and T) is then calculated as follows:

$$n_{DT} = n_e\left(1 - f_{imp} Z_{imp}\right) - 2n_{He}$$

The total particle density (volume average) is then:

$$n_{Total} = n_e + n_{DT} + n_{He} + n_{imp} = n_{DT}\left[\frac{\left(1+f_{imp}\right)}{\left(1-f_{imp}Z_{imp}\right)}+1\right] + n_{He}\left[\frac{2\left(1+f_{imp}\right)}{\left(1-f_{imp}Z_{imp}\right)}+1\right]$$

4.11 Separate Ion and Electron Power Balance

Global power balance equates the net total input power to the stored energy divided by the energy confinement time:

$$P_{Tot} = P_\alpha + P_{aux} - P_{rad} = P_\alpha + \frac{P_{fusion}}{Q} - P_{rad} = P_\alpha\left(1+\frac{5}{Q}-f_{rad}\right) = \frac{W}{\tau_E}$$

A toggle is provided in the calculations which is used to select whether T_i=T_e or not, in which case the ion and electron power balances are treated separately. For the case when they are treated separately, for the electrons:

$$P_{Tot\_e} = P_{\alpha\_e} + P_{aux\_e} - P_{rad} + P_{ie} = \frac{W_e}{\tau_{E\_e}}$$

where the "_e" notation denotes electron quantities, and P_{ie} is the power transfer from ions to electrons. Similarly for the ions:

$$P_{Tot\_i} = P_{\alpha\_i} + P_{aux\_i} - P_{ie} = \frac{W_i}{\tau_{E\_i}}$$

Note that the radiation term is included for the electrons only, and the P_{ie} term is additive for the electrons and subtractive for the ions. Solution of the above relies on expressions which estimate the partitioning of the alpha and auxiliary power to the ions and electrons, along with an expression for P_{ie}.

4.11.1 Neutral Beam Heating of Ions and Electrons

Including collisions with both electrons and background ions, the slowing down of a beam ion with energy E_{nbi} is given by:

$$\frac{dE_{nbi}}{dt} = -\frac{E_{nbi}}{\tau_{se}}\left[1 + \left(\frac{E_{crit}}{E_{nbi}}\right)^{1.5}\right]$$

where the first term in the square parenthesis is due to collisions with electrons, and the second term is due to collisions with ions, and τ_{se} is the slowing down time of electrons. For a deuterium beam injected into a 50/50 D-T plasma, the "critical" beam energy E_{crit} (at which the two contributions are equal) is given by Goldston and Rutherford [10]:

$$E_{crit} = 16T_e$$

More generally, in a D-T mix with a tritium fraction f_T, then the critical energy is:

$$E_{crit} = 29.5\frac{T_e}{M^{2/3}}$$

Where M is the average atomic mass number:

$$M = 3f_T + 2(1 - f_T) = f_T + 2$$

The auxiliary heating power density going into the electrons can be expressed in terms of an integral over beam energies, as follows:

$$P_{aux\_e} = \frac{P_{aux}}{E_{inj}} \int dE_{nbi} \left[1 + \left(\frac{E_{crit}}{E_{nbi}} \right)^{1.5} \right]^{-1}$$

where the integral runs from $E_{nbi} = 0$ to $E_{nbi} = E_{inj}$. This integral can be evaluated in the two limiting cases $E_{inj}/E_{crit} >> 1$ and $E_{inj}/E_{crit} << 1$, but these two limiting expressions are not very good at intermediate values of the parameter E_{inj}/E_{crit}, which are characteristic of actual CTF cases. We have evaluated the integral numerically for such cases, and we find that a good fit is given by the expression:

$$P_{aux\_e} = \frac{P_{aux}}{\left[1 + 2.9 \left(\frac{E_{crit}}{E_{inj}} \right)^{1.2} \right]}$$

which is accurate to within 2% over the range $E_{inj}/E_{crit} \approx 0.5 - 5.0$. Obviously it follows that:

$$P_{aux\_i} = P_{aux} - P_{aux\_e}$$

We calculate E_{crit}, P_{aux_i}, and P_{aux_e} as a function of T_e for each beam species and numerically integrate over the profile.

4.11.2 Alpha Heating of Ions and Electrons

Although alpha particles will heat mainly electrons, the small direct contribution to ion heating may be significant if the ion energy confinement time is very long. The derivation is similar to that for the beam ions presented above, and the alpha heating power density to electrons is given by:

$$P_{\alpha\_e} = \frac{P_{\alpha}}{E_{\alpha 0}} \int dE_{\alpha} \left[1 + \left(\frac{E_{crit}}{E_{\alpha}} \right)^{1.5} \right]^{-1}$$

where $E_{\alpha 0} = 3.5$ MeV, and the integration runs from $E_{\alpha} = 0$ to $E_{\alpha} = E_{\alpha 0}$. The alpha heating power density to ions is then given by:

$$P_{\alpha\_i} = P_{\alpha} - P_{\alpha\_e}$$

For alpha slowing-down in a 50/50 D-T plasma, we have:

$$E_{crit} = 32 T_e$$

More generally, in a D-T mix with a tritium fraction f_T and $M = f_T + 2.0$ the critical energy is:

$$E_{crit} = 59 \frac{T_e}{M^{2/3}}$$

The above integral for P_{α_e} can be evaluated in the limit $E_{\alpha 0} >> E_{crit}$. We obtain:

$$P_{\alpha\_e} = P_{\alpha}\left[1 - 2.4\frac{E_{crit}}{E_{a0}} + 2\left(\frac{E_{crit}}{E_{a0}}\right)^{1.5}\right]$$

Again, we calculate E_{crit}, P_{α_i}, and P_{α_e} as a function of T_e and numerically integrate over the profile.

4.11.3 Ion-Electron Equilibrium

The power per unit volume transferred from ions to electrons by Coulomb collisions in a 50/50 D-T plasma is given by:

$$P_{ie} = 0.55 n_{20}{}^2 \frac{\left(T_{i\_10} - T_{e\_10}\right)}{T_{e\_10}{}^{1.5}} \qquad (\mathrm{MW/m^3})$$

More generally, in a D-T mix with tritium fraction f_T and M= f_T +2.0, the power transfer is:

$$P_{ie} = \left(\frac{1.375}{M}\right) n_{20}{}^2 \frac{\left(T_{i\_10} - T_{e\_10}\right)}{T_{e\_10}{}^{1.5}} \qquad (\mathrm{MW/m^3})$$

where n_{20} is the (electron) density in units of 10^{20} m^{-3}, and each T_{10} is a temperature (simple temperature, not density weighted) in units of 10 keV, i.e., T_{10} = T(keV)/10. Again, we calculate P_{ie} as a function of ion and electron temperatures and numerically integrate over the profile.

4.12 Temperature

The ion and electron temperatures and densities are related to the pressure as follows:

$$P = nT\left(1.6 \times 10^{-19}\right)$$

with 1.6 x 10^{-19} Joule/eV.

We numerically integrate the ion and electron temperature, density, and pressure profiles to determine their peaking factors (PF, peak to average ratios) based on the specified functional forms. Then we know that:

$$< P >= \frac{\beta_N I_P B_T}{2\mu_0 a}$$

With PF_p and PF_n determined we can then back out the peak temperature as follows:

$$T_0 = \left(\frac{\beta_N \mathrm{I_p B_T}}{2\mathrm{R_0}\varepsilon\mu_0}\right)\left(\frac{\mathrm{PF_P}}{\mathrm{PF_n} * < n > * 1.6\mathrm{x}10^{-19}}\right)$$

The above calculation is performed separately for the ions and electrons.

4.13 Radiation

The effective ionic charge Z_{eff} is:

$$Z_{eff} = \frac{\sum_{ions} Z_j^2 n_j}{\sum_{ions} n_j Z_j} = \frac{\sum_{ions} Z_j^2 n_j}{n_e} = \frac{n_{DT} + 4n_{He} + Z_{imp}^2 n_{imp}}{n_e} = \frac{n_{DT} + 4n_{He} + Z_{imp}^2 f_{imp} n_e}{n_e}$$

Power loss (MW), assumed to arise exclusively from Bremsstrahlung radiation is:

$$P_{rad} \approx P_{brem} = 4.8 \times 10^{-43} Z_{eff} n_e^2 \sqrt{T} a^2 R_0 \kappa \left[\frac{(1+\alpha_N)^2 (1+\alpha_T)^{1/2}}{1 + 2\alpha_N + \frac{1}{2}\alpha_T} \right]$$

4.14 Alpha Power

4.14.1 Thermal Ion Fusion

Alpha power due to "thermal" ions in a 50:50 D-T mix is calculated per the following integral from Hively [11]:

$$P_{\alpha 50:50} = 5.6 \times 10^{-25} \int_0^{V_p} \left[n_{DT}^2(V) e^{a_0 + a_* T(V)^{-0.275} + a_1 T(V) + a_2 T(V)^2 + a_3 T(V)^3} \right] dV$$

where:

a_0 = -23.836
a_* = -22.712
a_1 = -0.09393
a_2 = 7.994e-4
a_3 = -3.144e-6

More generally, in a D-T mix with tritium fraction f_T:

$$P_\alpha = P_{\alpha 50:50} 4 f_T (1 - f_T)$$

4.14.2 Two-Component Beam-Target Fusion

The basic data on the energy-multiplication factor Q_{TC} for "two-component" reactions between injected deuterium ions and a pure-tritium background plasma is based on work by Jassby [12] which gives data for temperatures up to 20 keV for cases with $T_i = T_e$, as well as data for T_e = 50 keV and T_i = 0, to which an approximate finite-T_i correction fit can be applied. Curve fits were generated to match figure 18 from the Jassby paper for $T_i = T_e$ and to extend the curves from 400keV out to 1MeV. These are applied to the work

reported herein despite the fact that the $T_i = T_e$ equality is not enforced. This is justified on the basis that the primary dependency is on T_e alone. For E_b up to 400keV the equation form is based on that in the NRL Plasma Formulary [13] which uses the Duane coefficients to compute fusion cross sections:

$$\sigma_T(E) = \frac{A_5 + \left[(A_4 - A_3 E)^2\right]^{-1} A_2}{E\left[\exp\left(A_1 E^{-1/2}\right) - 1\right]}$$

This was modified as follows:

$$\sigma_T(E) = \frac{A_0 E\left\{A_5 + \left[(A_4 - A_3 E)^2\right]^{-1} A_2\right\}}{\left[\exp\left(A_1 E^{-1/2}\right) - 1\right]}$$

The modification brings the form closer to that associated with the calculation of Q_b as reported by Jassby, and was found to provide very tight fits with the Jassby figure. In order to cover the range of T_e it was necessary to use another level of curve fitting for the coefficients A_1 through A_5 as a function of T_e . The equation form used was:

$$A_x(T) = A_{x0} T^{A_{x1}}$$

The coefficients were determined by least squares curve fitting to the set of points taken manually from the Jassby figures. The results are given in table 1.

Table 1. Beam-target fusion coefficients

A0	0.0010
A10	51.713
A11	-0.191
A20	50202.423
A21	1.483
A30	0.009
A31	0.417
A40	-0.250
A41	1.164
A50	-1323.179
A51	0.144

In order to extend the results out to 1MeV it was assumed that Q should go roughly as $Q_{b\_E>400keV} = Q_{b\_E=400keV} * 400 / E_b$. Curve fit results are shown in figure 6.

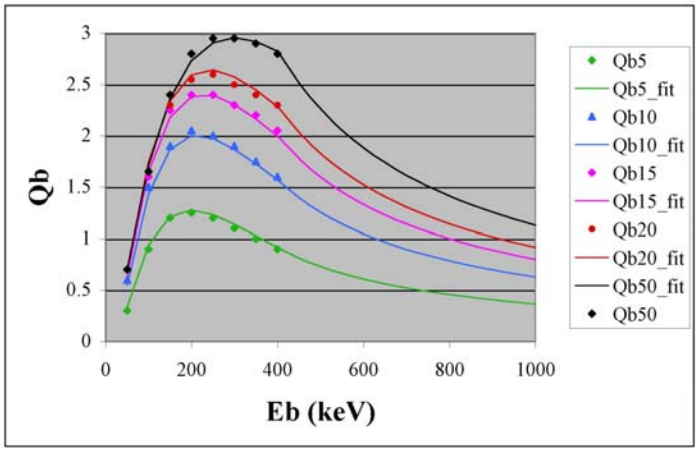

Figure 6. Fits to beam-target energy multiplication curves

The total fusion power from two-component reactions due to NBI into a 50:50 DT mix is obtained by integrating over the plasma volume:

$$P_{f\_TC} = \frac{1}{2}\int Q_{TC}(r)P_{nbi}(r)dV$$

Where the factor 1/2 arises from the fact that only 50% of the target ions are of the species opposite to the injected species.

4.14.3 Integration of Fusion Power Over Plasma Volume

As depicted in figure 7, the incremental volume ΔV is:

$$\Delta V = \kappa\left[2\pi R_0\right]\left[2\pi R\right]\Delta R$$

where R is the radius from the plasma center at $R_{0.}$

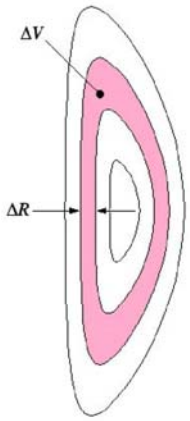

Figure 7. Profile Integration

4.15 Plasma Stored Energy

The plasma thermal energy is:

$$W = \frac{3}{2} < P > V = \frac{3}{2}\left[\frac{\beta_N 10^{-6} I_P B_T}{2\mu_0 a}\right]\left[2\pi^2 R_0 a^2 \kappa\right]$$

4.16 Energy Confinement Time

Three versions of the energy confinement time are calculated, namely neoclassical, ITER 89 scaling, and ITER 98[y,2] scaling [14]. When the calculations are performed in the mode where $T_i=T_e$, the ITER 98[y,2] scaling is used for the ions and electrons. Otherwise the ion confinement is assumed neoclassical and the electrons per ITER 98. The ITER 89 scaling is calculated and reported but not otherwise used.

For the ITER 98[y,2] scaling:

$$\tau_E^{98[y,2]} = \left[0.0562 M^{0.19} I_p^{0.93} R_0^{1.97} B_T^{0.15} \varepsilon^{0.58} \kappa_a^{0.78} \overline{n}_{e19}^{0.41} / P_{Tot}^{0.69}\right]$$
$$= \left[\frac{0.0562 M^{0.19} I_p^{0.93} R_0^{1.97} B_T^{0.15} \varepsilon^{0.58} \kappa_a^{0.78} \overline{n}_{e19}^{0.41}}{\left(P_\alpha\left(1 + 5/Q - f_{rad}\right)\right)^{0.69}}\right]$$

where $\overline{n}_{e19}$ is the line average electron density in units $10^{19}/m^3$ and M is the average mass number, equal to 2.5 for a 50:50 DT mix.

For the ITER 89 scaling:

$$\tau_E^{89} = \left[0.048 I_p^{0.85} R_0^{1.2} B_T^{0.2} a^{0.3} \kappa_a^{0.5} \overline{n}_e 20^{0.1} M^{0.5} / P_{Tot}^{0.5}\right]$$
$$= \left[\frac{0.048 I_p^{0.85} R_0^{1.2} B_T^{0.2} a^{0.3} \kappa_a^{0.5} \overline{n}_e 20^{0.1} M^{0.5}}{\left(P_\alpha\left(1 + 5/Q - f_{rad}\right)\right)^{0.5}}\right]$$

To develop a simple approximation for the neoclassical ion energy confinement time it is important to take aspect ratio effects into account, since the approximation a/R << 1, which may be valid for tokamaks, is certainly not adequate for STs. However, it is less important to take account of neoclassical regimes other than the lowest-collisionality "banana" regime, since the topic is of interest only for high-T_i cases where the parameter ν_{*i} is very small. The neoclassical formulation most suited to this case is that by Chang and Hinton [15], and we use this formulation for the ion thermal conductivity χ_i.

In an actual case, even when χ_i is given, the energy confinement time will depend on the profile of net heating power. For present purposes, we choose to ignore this dependence and simply obtain a generic characteristic expression for the ion energy confinement time τ_{Ei}. We do this by assuming an essentially constant χ_i and then treating the heat transport equation as if it were a diffusion equation of the form $D\nabla^2 T + T/\tau_{Ei} = 0$ which, for cylindrical geometry, has Bessel functions $J_0(\lambda r)$ as solutions with the eigenvalue τ_{Ei} then arising from setting $\lambda a = 2.4$, i.e., the first

zero of J_0. For the "constant" value of χ_i, we take the actual value evaluated at r/a = 0.5, assuming the reference plasma profiles. We assume an aspect ratio R/a = 1.5 so that χ_i is calculated at r/R = 0.33 (the parameter δ in the Chang/Hinton paper). We assume a 50/50 D/T plasma.

On this basis, we obtain the following final expression for the ion energy confinement time:

$$\tau_{Ei}^{NC} = \frac{0.11 C_\kappa C_{Zeff} C_{plat} I_p^2 \langle T_i \rangle^{0.5} A^{0.5}}{\langle n_{20} \rangle}$$

Here, I_p is the plasma current in MA, $<T_i>$ is the average ion temperature in keV, $<n_{20}>$ is the average density in units of 10^{20} m^{-3}, and A = R/a is the aspect ratio. The factors C_κ, C_{Zeff} and C_{plat} are correction factors to take into account the effects of elongation, impurities and the banana-plateau transition, respectively.

The neoclassical confinement time in the banana regime goes like the square of the poloidal flux within the plasma. As the elongation is increased at fixed toroidal field and fixed q-value, the poloidal flux increases, but so does the plasma current, with the result that most of the effect of elongation is already included in the above formula through the dependence on I_p. In fact, the plasma current increases with elongation somewhat more rapidly than the poloidal flux, with the result that a correction factor:

$$C_\kappa = \left[\frac{2\kappa}{\left(1+\kappa^2\right)} \right]^2$$

should be applied. This correction factor will be important only at fairly large elongation.

Simplistically, the effect of impurities would be taken into account by simply increasing the ion-ion collision frequency by Z_{eff}, which would correspond to $C_{Zeff} = Z_{eff}^{-1}$. However, a later paper by Chang and Hinton [16] shows that impurities typically have a stronger effect on the transport because the impurity ions tend to be in a higher collisionality neoclassical regime. These results can be approximated by taking:

$$C_{Zeff} = \left[1 + 2.4\left(Z_{eff} - 1\right) \right]^{-1}$$

Most cases of interest would seem to be deeply into the banana neoclassical regime, since the value of ν_{*i} is very small. However, if banana-plateau transition effects are significant, they would tend to increase the confinement time by a small factor. The Chang/Hinton paper gives a correction factor:

$$C_{plat} = 1 + \nu_{*i}^{0.5} + 0.3\nu_{*i}$$

and a representative value of ν_{*i} is given by:

$$\nu_{*_i} = \frac{0.02 Z_{eff} \langle n_{20} \rangle q R_0 \left(\frac{R_0}{a} \right)^{1.5}}{\left\langle T_i \right\rangle^2}$$

4.17 Confinement Enhancement Factor

A confinement enhancement factor HH is introduced and used in the power balance equations as follows:

$$HH = \frac{W}{\tau_E P_{Tot}} = \frac{W}{P_\alpha \left(1 + \frac{5}{Q} - f_{rad} \right)}$$

So, the effective confinement time is:

$$\tau_{E\_eff} = HH * \tau_E$$

4.18 Fast Ion Effects

In addition to the pressure resulting from the "thermal" DT ions, additional partial pressures result from the alpha particles and the beam ions. These all add to the pressure which is taken into account in determining the total effective beta values which are compared by the solver to the allowable beta limits.

4.18.1 Alpha contributions

An individual alpha-particle will give up its energy E_α according to the relation $dE_\alpha/dt = -E_\alpha/\tau_{slow\_\alpha}$, where τ_{slow_α} is the energy "slowing-down" time due to collisions with electrons. If P_α is the alpha-particle heating power density in MW/m^3, the stored energy density in alphas is then given by:

$$W_{stored\_\alpha} = P_a \tau_{slow\_\alpha}$$

The energy slowing-down time for alpha particles is given by:

$$\tau_{slow\_\alpha} = 0.18 \frac{A_\alpha T_{10}^{1.5}}{Z_\alpha^2 n_{20}} = 0.18 \frac{T_{10}^{1.5}}{n_{20}}$$

where T_{10} is the electron temperature in units of 10 keV, and n_{20} is the electron density in units of 10^{20} m^{-3}. (For alphas, atomic mass $A_\alpha = 4$ and charge $Z_\alpha = 2$. In the underlying physics, we have taken $\ln \Lambda \approx 18$.)

We calculate the stored energy as a function of density and temperature and numerically integrate over the profile.

With the stored energy density in MJ/m^3 and the toroidal field strength in Tesla, the alpha contribution to toroidal beta is:

$$\beta_{T\_\alpha} = \frac{1.68\langle W_{stored\_\alpha}\rangle}{B_T^2}$$

4.18.2 Beam ion contributions

Including collisions with both electrons and background ions, the slowing down of a beam ion with energy E_b is given by:

$$\frac{dE_{nbi}}{dt} = \frac{-E_{nbi}}{\tau_{slow\_nbi}}\left(1 + \frac{CT_e^{1.5}}{E_{nbi}^{1.5}}\right)$$

where the second term in the parenthesis on the right is due to collisions with ions. For a deuterium beam injected into a 50/50 D/T plasma, the constant C ≈ 64 (see Goldston and Rutherford [10]. Thus, for electron temperatures in the range 10-15 keV, the "critical" beam energy E_{crit} (at which the two contributions are equal) is in the range 160-240 keV. Above E_{crit}, the beam ions will slow down mainly by collisions with electrons and, below this energy, mainly by collisions with ions. From the above expression for dE_{nbi}/dt, the equilibrium "slowing-down" velocity distribution of beam ions can be derived. Multiplying by beam energy and integrating over all velocities, the stored energy density in the beam ions can be obtained. However, the integrals cannot be done analytically except in the two limiting situations where electron collisions or ion collisions are by far predominant. A simple formula for the beam stored energy that fits exactly to these two limiting cases, and which is expected to be reasonably good in intermediate cases also, is as follows:

$$W_{stored\_nbi} = \frac{P_{nbi}\tau_{slow\_nbi}}{\left[1 + 2.5\left(\frac{E_{crit}}{E_{nbi}}\right)^{1.5}\right]}$$

Here, E_{nbi} is the beam injection energy and τ_{slow_nbi} is the slowing-down time for beam ions by electron collisions, given by:

$$\tau_{slow\_nbi} = 0.18\frac{A_{nbi}T_{10}^{1.5}}{Z_{nbi}^2 n_{20}} = 0.36\frac{T_{10}^{1.5}}{n_{20}}$$

We calculate the stored energy as a function of density and temperature and numerically integrate over the profile. Finally, the beam contribution to toroidal beta is:

$$\beta_{T\_nbi} = \frac{1.68\langle W_{stored\_nbi}\rangle}{B_T^2}$$

5. Engineering Algorithms

In this section we present engineering algorithms in two parts. First for a pulsed experimental NSTX-like device with copper magnets and second for a CTF-like steady state D-T reactor.

5.1 Engineering Algorithms for Pulsed Copper Machine

We are concerned with the heating and mechanical stress in the coils located in the narrow central core of the device, as well as the flux available to induce plasma current.

5.1.1 Waveform Assumptions

As shown in figure 8, we assume a pulsed scenario where the central solenoid (CS) is driven as rapidly as possible to an initial value of current, then ramped through zero to generate plasma current up to the "start of flat top" (SOFT), then (if we assume solenoid flux is required during plasma flat top) further ramped until the "end of plasma flat top" (EOFT), then ramped down. Ramp rates are specified according to typical operating experience. We assume that the TF coil is driven as rapidly as possible to flat top current, then held at flat top for the full duration of plasma current, such that the TF is at full field for the entire non-zero plasma current duration. Rise times for the CS and TF are based on L-R circuit behavior with realistic power supply parameters.

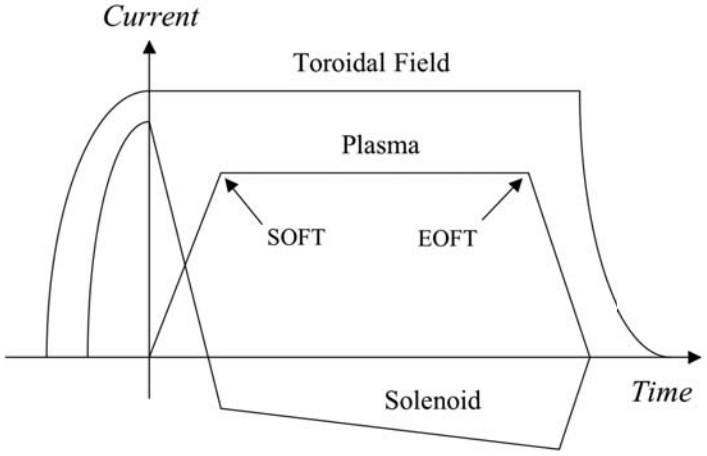

Figure 8. Current waveforms for pulsed machine

The XL solver calculates the J^2T integrals of the above TF and CS waveforms and can adjust, among other things, the values of first swing and second swing CS currents in order to optimally satisfy the demand for magnetic flux while not overheating or overstressing the conductor.

5.1.2 Conductor Heating

We use the "G" function approach described as follows, and develop it for both copper and beryllium copper conductor materials.

Let:

ρ_e = electrical resistivity
ρ_{e0} = electrical resistivity at temperature t_{0e}
T = temperature
α = temperature coefficient of resistivity
$\rho_e = \rho_{e0}(1+\alpha(T-T_0))$
ρ_d = density
C_p = specific heat = f(T)
J = current density
t = time

Then for an adiabatic conductor:

$$\rho_e J^2 dt = \rho_d C_p dT$$

Rearranging and integrating results in the G function:

$$J^2 dt = \int \frac{\rho_d C_p dT}{\rho_e} \equiv G(T)$$

Curve fits were used to develop G functions for Cu and BeCu over the temperature range 80°K to 473°K (200°C). These are of the form:

$$G(T) = g_0 + g_1 T + g_2 T^2 + g_3 T^3$$

Coefficients are given in table 2.

Table 2. Coefficients for G Function

	Cu	BeCu
g0	-5.641e16	-1.681e16
g1	8.859e14	2.169e14
g2	-1.963e12	-1.498e11
g3	1.779e9	3.760e7

On this basis the conductor current density J which is allowable given a temperature limit T can be determined as follows:

$$J = \sqrt{\frac{G(T_{allow}) - G(T_0)}{T_{ESW}}}$$

Within the conductor pack the packing fraction is defined as follows:

$$K_{pf} = \frac{A_{conductor}}{A_{total}}$$

Then the current density has an average value of:

$$J_{avg} = JK_{pf}$$

The G function can also be used to estimate the temperature of the conductors at any value of J^2t as follows:

$$\Delta G = \int J^2(t)$$
$$G = G(T_o) + \Delta G$$

Curve fits were used to develop inverse G functions for Cu and BeCu. These are of the form:

$$T(G) = xg_0 + xg_1 G + xg_2 G^2 + xg_3 G^3$$

Coefficients are given in table 3.

Table 3. Coefficients for G^{-1} Function

	Cu	BeCu
xg0	82.96	81.45
xg1	9.020e-16	5.371e-15
xg2	1.794e-32	6.918e-33
xg3	5.585e-50	3.769e-49

5.1.3 Mechanical Stress in Coils

a. Central Solenoid

We estimate via Roark & Young [17] the peak hoop stress in the solenoid which occurs at the bore as follows:

$$\sigma = JB\left\{\begin{array}{l}\dfrac{(7+5\nu)R_0^4 - 8(2+\nu)R_0R_i^3 + 3(3+\nu)R_i^4}{24(R_0-R_i)(R_0^2-R_i^2)} \\ -\dfrac{(1+2\nu)R_0R_i}{3(R_0-R_i)} + \dfrac{(1+3\nu)R_i^2}{8(R_0-R_i)} \\ +\dfrac{R_0^2\left[(7+5\nu)R_0^2 - 8(2+\nu)R_0R_i + 3(3+\nu)R_i^2\right]}{24(R_0-R_i)(R_0^2-R_i^2)}\end{array}\right\}$$

where:

R_o = outer radius of conductor pack
R_i = inner radius of conductor pack
ν = Poisson's Ratio

Here B is the (constant) field within the bore of the coil:

$$B = \mu_0 J_{avg}(R_o - R_i) * ff$$

Where ff is the form factor which accounts for the finite length ΔZ of the coil:

$$ff = \frac{\Delta Z}{\sqrt{\Delta Z^2 + \left[\dfrac{(R_o + R_i)}{2}\right]^2}}$$

We limit the peak stress to an appropriate allowable value. Note that a more rigorous approach would calculate combined stress (e.g. Von Mises or Tresca) including effects from nearby PF coils and the plasma. However, the approach described is considered adequate for parametric studies.

b. Toroidal Field Inner Leg

We consider the stresses arising from the axial current flow in the bundle, and assume that forces generated on the radial currents in the outer return path are shunted from the inner leg by dedicated mechanical support structures. Tri-axial and combined (Von Mises) stresses are computed as follows:

$$\sigma_{rr} = \left(-\frac{B_{\max}{}^2}{2\mu_0}\right)\left(\frac{3-2\nu}{2(1-\nu)}\right)\left(1-\left(\frac{r}{a}\right)^2\right)$$

$$\sigma_{\varphi\varphi} = \left(-\frac{B_{\max}{}^2}{2\mu_0}\right)\left(\frac{3-2\nu}{2(1-\nu)} - \frac{1+2\nu}{2(1-\nu)}\left(\frac{r}{a}\right)^2\right)$$

$$\sigma_{zz} = \left(-\frac{B_{\max}{}^2}{2\mu_0}\right)\left(\frac{\nu}{1-\nu}\right)\left(1-2\left(\frac{r}{a}\right)^2\right)$$

$$\sigma_{VonMises} = \sqrt{\frac{\left(\sigma_{rr}-\sigma_{\varphi\varphi}\right)^2+\left(\sigma_{\varphi\varphi}-\sigma_{zz}\right)^2+\left(\sigma_{zz}-\sigma_{rr}\right)^2}{2}}$$

where:

r = radius within conductor
a = outer radius of conductor
ν = Poission's ratio
B_{max} = B at r=a, $B_{max} = \mu_0 I_{TF}/2\pi a$

We note that the shear in the insulation between turns due to torsion arising from JxB forces between TF current and CS radial field can be an important and limiting factor. However we have not developed an algorithm for it at this time since it involves the structural support system and is probably too complex to represent in parametric studies.

5.1.4 Solenoid Flux Requirement

The formulation developed by Hirshman and Neilson [18] is used to estimate the flux requirement of the central solenoid:

$$\Delta\psi = \mu_o R I_p (l_{ext} + \frac{l_i}{2} + C_E + C_{flat}\Delta t_{flat})$$

$$C_{flat} = .02\left(\frac{T_{0e}}{10}\right)^{-1.5}\frac{Z_{eff}}{1.4}$$

$$l_{ext} = l_s - (m/4)[\ln(8/\varepsilon\sqrt{\kappa}) + \beta_p + l_i/2 - 1.5]$$
$$l_s = a_1(1-\varepsilon)/(1-\varepsilon+a_2\kappa)$$
$$m = (1-\varepsilon)^2/[a_3(1-\varepsilon)^2 + a_4\sqrt{\kappa}]$$

where:

l_i is the "energy based" internal self-inductance
Δt_{flat} is the flattop time
C_E is the Ejima coefficient

and:

$$a_1 = (1+1.81\sqrt{\varepsilon}+2.05\varepsilon)*\ln\left(\frac{8}{\varepsilon}\right) - (2+9.25\sqrt{\varepsilon}-1.21\varepsilon)$$
$$a_2 = 0.073\sqrt{\varepsilon}(1+2\varepsilon^4-6\varepsilon^5+3.7\varepsilon^6)$$
$$a_3 = 1+0.98\varepsilon^2+0.49\varepsilon^4+1.47\varepsilon^6)$$

$$a_4 = 0.25\varepsilon(1 + 0.84\varepsilon - 1.44\varepsilon^2)$$

Note that the above is the flux required from the central solenoid, and excludes the flux arising from the vertical field necessary for plasma equilibrium. Depending on the assumptions specified for non-inductive current drive, the solver sets the solenoid flux requirement to some fraction of the ramp and flat top flux as computed above.

5.2 Engineering Algorithms for Reactor

For a steady state reactor (e.g. CTF) we assume a solenoid-less configuration with single turn TF, non-inductive current drive using NBI, high power divertor exhaust, tritium (T) breeding blanket, and electricity production.

5.2.1 First Wall and Toroidal Field Inner Leg

The first wall thickness requirement ΔR_{fw} is driven by compromises between ohmic power dissipation, nuclear heating, and neutron damage to the center post (and frequency of replacement). For the work reported herein the thickness was assumed 6 cm for the CTF mission based on the Culham VNS study[19], and 20cm for reactor missions based on the ARIES-ST study[20], so the radial build of the TF inner leg in the midplane region is:

$$R_{TFmid} = R_0 - a_{100} - \Delta R_{fw}$$

The radius of the inner leg in the end regions was set to:

$$R_{TFend} = R_{TFmid} + a_{100}(1 - \delta)$$

The height of the narrow middle region of the inner leg above the midplane is assumed equal to 90% of the height of the plasma.

$$\Delta Z_{TFmiddle} = 0.9 * \kappa * a_{100}$$

The total TF height is taken to be equal to the plasma height plus 4.0m, allowing for divertor, blanket, and shield:

$$\Delta Z_{TF\,max} = \kappa * a_{100} + 4.0m$$

Glidcop AL-25 material, σ=87% IACS, was assumed for the inner leg, based upon its radiation resistance, consistent with the ARIES-ST. The inner leg is modeled using 8 sections as depicted in figure 9, with water flowing in one end and out the other, heating up as the sections are traversed.

A water inlet temperature of 35ºC and flow velocity of 10m/s were assumed. The fraction of cross section containing water is chosen by the optimizer. The number of water passages per unit area is assumed equal to 500/m^2, similar to ARIES-ST, but less than prior VNS [21] studies which were of order 2000/m^2. Thus with the water cross sectional area and number of passages specified the wetted perimeter of the cooling passages is determined.

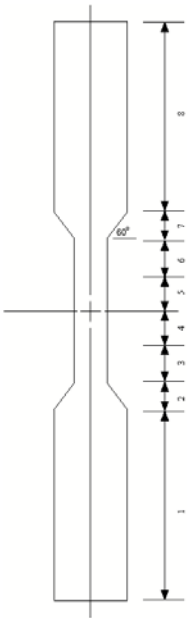

Figure 9. TF Inner Leg

In addition to ohmic dissipation, nuclear heating is added at a rate equal to the average neutron wall loading times the surface area. This is conservative because 1) much of the heating would be received and removed or radiated via the first wall armor, and 2) the Cu is partially transparent to the neutrons. The flaring is set to 60º with respect to horizontal, with the flaring starting at 90% of the plasma height.

The thermal resistance due to the film effect and the mass flow are computed, using water properties which are computed as a function of temperature. Limits on copper and water temperature were typically set at 150ºC.

Stresses in the inner leg are computed using the same formulation as for the pulsed machine. Vertical tension is assumed equal to zero, which is consistent with the use of sliding joints at the interface between the vertical center post and radial current paths to the return circuit. However the above result was multiplied by a factor of 2.0 to account for the cooling passages in the conductor. An appropriate limit for Glidcop at 150ºC is 100MPa.

5.2.2 Toroidal Field Outer Leg Return

As depicted in figure 10 the TF current is assumed to be returned through the outer VV shell which is constructed of aluminum, consisting of horizontal lids and vertical cylindrical sections. This is similar in concept to the VNS and ARIES-ST designs. The thickness of the horizontal sections and vertical sections is set to 0.6m.

Dimensions of the outer leg return circuit are chosen based on the following radial builds beyond the outboard plasma edge:

SOL and gap	0.10m
First wall	0.05m
Blanket	0.5m
Shield	0.7m
Gap	0.1m

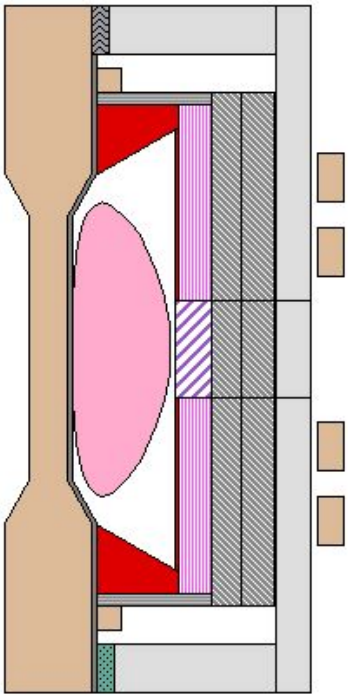

Figure 10. TF Cross Section, showing Inner Leg, Outer Leg Return, and Space Allocation for First Wall /Blanket/Shield (R_0=1.5m,A=1.5,κ=3.0,δ=0.4)

Dimensions are similar to those used for ARIES-ST, and are sufficient to handle 7.5MW/m^2 neutron flux on the outboard midplane and to protect the organic insulating materials of the outer PF coils. For a CTF with lower power flux and lower fluence, a shield thickness of approximately 1.0m would be required to permit hands-on access. Future work should address this issue and determine the optimum shielding considering the actual CTF loading scenarios and access requirements related to the use of blanket test modules.

5.2.3 Determination of Toroidal Field, Current, Input Power

The optimizer adjusts the current density in the TF inner legs along with the fraction of cross-sectional area containing water (f_W) to adjust B_T according to:

$$I_{TF} = J_{TF}\pi R^2{}_{TFmid}\left(1 - f_W\right)$$

$$B_T = \frac{\mu_0 I_{TF}}{2\pi R_0}$$

Total TF power consumption is equal to the sum of the dissipation in the inner and outer legs divided by the efficiency of the power supply system, assumed to be 90%:

$$P_{TF} = \frac{P_{inner} + P_{outer}}{\eta_{TF}}$$

Further work is needed to establish the details of the ultra-high current TF power supply and confirm that reasonable efficiencies can be obtained.

5.2.4 Poloidal Field Requirements

A switch in the spreadsheet is used to select copper PF coils or superconducting. If copper, their total current is assumed equal to the plasma current. Current density is assumed to be $J_{PF} = 5.0 \times 10^6$ amp/m^2. Their inboard edge is assumed to be 0.4m beyond the outboard edge of the VV. Power supply efficiency is taken to be 95%. With these assumptions the power dissipation in the PF coils is computed.

$$P_{PF} = \frac{I_P^2 \rho 2\pi R_{PF}}{A_{PF}\eta_{PF}} = \frac{I_P J_{PF} \rho 2\pi R_{PF}}{\eta_{PF}}$$

If superconducting the PF input power is assumed equal to zero. Refrigeration power requirements are assumed lumped with balance of plant power.

5.2.5 Divertor and First Wall Heat Loads

The power in the scrape-off layer is:

$$P_{SOL} = P_\alpha + P_{aux} - P_{brem} - P_{line}$$

For the work described herein the cyclotron radiation is neglected and the line radiation is assumed equal to the bremsstrahlung radiation plus additional radiation of the power leaving the core of the plasma via Ar introduced into the core to enhance radiation.

Algorithms to estimate the divertor heat loads were developed from equilibrium calculations. The divertor configuration flux expansion, for reasonable divertor geometry assumptions, is found to follow:

$$\lambda_{div} = \lambda_{midplane} \times 7.5a$$

where a is the minor radius, and λ is the e-folding of the heat flux in the scrape off layer. Then the power into the scrape off layer can be related to the peak heat flux by

$$P_{SOL} = Q_{div} \times 4\pi(R + \frac{a}{4})\lambda_{div}$$

where Q is the peak heat flux This is assuming particle heat load only. If we now include radiation in the divertor, we get two terms, and solving for the peak heat flux:

$$P_{div} = P_{SOL} - P_{div,rad}$$

$$Q_{div} = P_{div,rad}/(8\pi Ra) + P_{div}/[4\pi(R + \frac{a}{4})\lambda_{div}]$$

Note that the $8\pi Ra = 2(2\pi R)2a$ is the divertor area, based on actual geometric layout studies. The inputs are the midplane scrape off layer e-folding at the midplane (assumed equal to 1.0cm) and the divertor radiation fraction. In addition, to the calculation of the peak heat flux in the divertor, we must calculate the surface heat flux on the first wall, since its capability is typically much less than the divertor. So the first wall heating is given by…

$$P_{FW} = P_{brem} + P_{line}$$
$$Q_{FW} = P_{FW} \times f_{peaking} / A_{FW}$$

The solver equations are designed to adjust the radiation fraction at the divertor as well as the core radiation to suit the engineering allowable peak heat flux. Solver solutions are valid if both the divertor peak heat flux and the first wall heat flux are within limits. The following constraints are typically applied:

Allowable peak heat flux at divertor = 15.0 MW/m^2
Maximum radiation fraction at divertor = 90%
Allowable peak heat flux at first wall = 1.0 MW/m^2
Maximum core radiation fraction = 60%
Minimum core radiation fraction = 60%

5.2.6 Neutron Wall Loading

Average neutron wall loading is based on the surface area of the plasma:

$$X_{N\_wall} = \frac{P_N}{A} = \frac{4P_\alpha}{4\pi^2 R_0 a\sqrt{(1+\kappa/2)}}$$

5.2.7 Blanket Coverage

The area available to the blanket is reduced by ports which are required for NBI and other purposes. It is assumed that tangential NBI ports are located on the midplane and that tangential injection is accomplished via horizontal beam lines. In addition it is assumed that one radial port each is reserved for RF and Diagnostics. Other ports which can contain blanket test modules are assumed radial and of the same dimensions as the RF and Diagnostics ports. It is assumed that all of the midplane ports have the same height which is taken to be at least 1.0m, or:

$$\Delta z_{port} = \min\left\{2\left(\frac{\kappa R_0}{A} - 1.5\right), \frac{2\kappa R_0}{3A}\right\}$$

The preferred port height, 1/3 of the plasma height, is judged to be a reasonable value which provides significant access to the high neutron flux zone of the plasma. However, in recognition of the need for remote handling access to the port flanges for cask attachment, etc., it is judged prudent to reserve 1.5m from the top of the plasma (where an outer PF coil will be located) to the top of the port.

5.2.7.1 NBI Port Requirements

For the high energy NBI envisioned ($E_{nbi} > 200$keV) negative ion injection methods are required, and the current density achievable through the NBI duct is assumed limited to $J_{nbi}=40 A/m^2$. This is based on JT-60 experience [22] with negative ion NBI which has targeted 10MW injection at 500keV through a duct of dimensions 1.1m x 0.45m. Knowing the NBI power and energy (equal to voltage for D and T ions) the total duct area and width can be determined as follows:

$$A_{nbi} = \frac{P_{nbi}}{E_{nbi} J_{nbi}}$$

and:

$$w_{duct\_total} = \frac{A_{nbi}}{\Delta z_{port}}$$

A maximum NBI duct width of 1.25m is assumed. Then the minimum number of NBI ports is:

$$N_{nbi} = \text{int}\left\{1 + \frac{w_{duct\_total}}{w_{duct\_\max}}\right\}$$

and the actual duct width is:

$$w_{duct} = \frac{w_{duct\_total}}{N_{nbi}}$$

From simple geometry considerations, and assuming that the NBI aims at R_0, it can be shown that the tangency angle, chord and angle corresponding to the NBI duct at the outboard first wall radius, assuming 15 cm gap from outboard edge to first wall are:

$$R_{ofw} = R_0 + a + 0.15m$$

$$R_{\tan} = R_0$$

$$\theta_{\tan} = \cos^{-1}\left\{\frac{R_{\tan}}{R_{ofw}}\right\}$$

$$C_{nbi} = \frac{W_{duct}}{\cos(\pi/2 - \theta_{\tan})}$$

$$\theta_{nbi} = 2\sin^{-1}\left\{\frac{C_{nbi}}{2R_{ofw}}\right\}$$

5.2.7.2 Radial Port Allocations and Dimensions

It is assumed from practical considerations that all radial ports are 1.0m wide, such that the angle corresponding to each port is:

$$\theta_{port} = 2\sin^{-1}\left\{\frac{1}{2R_{ofw}}\right\}$$

From the above, the maximum number of radial ports can be determined:

$$N_{port} = \text{int}\left\{\frac{360 - N_{nbi}\theta_{nbi}}{\theta_{port}}\right\}$$

If two ports are reserved to RF and Diagnostics, then the remaining ports would be available, e.g., to blanket test modules, and the total available blanket test module area would be:

$$N_{tm\_\max} = N_{port} - 2$$

$$A_{tm\_\max} = N_{tm\_\max}\Delta z_{port}\Delta w_{port}$$

5.2.8 Neutron Flux Distribution and Area Weighting

a. Center Stack

The fraction of neutrons incident on the narrow midplane region of the center stack is:

$$f_{CS} = \frac{\phi * \sin\theta}{2\pi}$$

where ϕ and θ are angles in the toroidal and poloidal planes which correspond to the intersection of a cylinder (the center stack) and a unit sphere with center at the effective average point source of neutron production, which is assumed located a distance a/3 beyond R_0. See figure 11. The angles ϕ and θ are:

$$\phi = \frac{2\sin^{-1} R_{fw}}{R_0 + a/3}$$

$$\theta = \frac{\tan^{-1}\left(\Delta Z_{tfmid}/2\right)}{\left(R_0 + a/3\right) - R_{fw}}$$

where R_{fw} is the radius of the first wall and ΔZ_{tfmid} is the height of the narrow midplane section of the center stack.

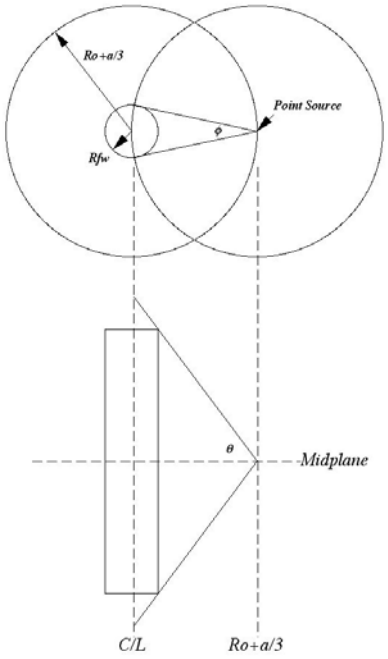

Figure 11. Calculation of Solid Angle of Center StackOutboard Blanket

b. Data from the ARIES-ST studies [23] by El Guebaly provide neutron flux distribution on a cylindrical blanket extending up to the plasma height κ*a, in terms of normalized neutron flux as a function of normalized height. The former normalization is w.r.t. machine average n flux (based on the total plasma facing surface), the latter w.r.t. plasma height. In addition from the ARIES-ST studies (A=1.6) the ratio of the neutron flux on the outboard blanket was equal to 4.6/3.3=1.39 times the machine average, with the machine average based on the total plasma facing surface. This information was used to estimate neutron flux distribution and weighting functions as follows.

The data from El Guebaly was scaled and curve fit to the following function:

$$n_{ob}(z) = 1.4318\left(1 - \frac{z}{1.016}\right)$$

This function has an integral of 1.0, which means that it represents the flux as a function of z, normalized to the average over the cylindrical blanket.

c. Overall Accounting of Neutron Flux

The total plasma facing surface area A_{pfs} is assumed to consist of that of a cylinder of height z=+/-κ*a at the outboard first wall radius A_{cyl}, a center stack represented by a cylinder down the middle at the inboard first wall radius A_{cs}, and lids top and bottom representing the divertor regions A_{div}.

Given the prior result concerning the fraction of neutron flux incident on the center stack f_{cs}, a weighting function applied to the center stack area is:

$$W_{cs} = f_{cs}\frac{A_{pfs}}{A_{cs}}$$

Similarly, for the cylindrical outboard blanket, given the ARIES ratio of 1.39,

$$W_{cyl} = 1.39\frac{A_{pfs}}{A_{cyl}}$$

Finally, for the divertor regions since $\sum W_i A_i/A_{pfs} = \sum A_i/A_{pfs} = 1.0$:

$$W_{div} = \frac{A_{pfs} - W_{cs}A_{cs} - W_{cyl}A_{cyl}}{A_{div}}$$

d. Neutron Flux to Blanket and Test Modules

With the weighting functions established, the equation for neutron flux to the outboard region can be modified to reflect same as follows:

$$\overline{n_{ob}}(z) = 1.4318W_{cyl}\left(1 - \frac{z}{1.016}\right)$$

This function gives the weighted flux dependency on z. For the radial ports which extend up to $z=+/-\Delta Z_{port}/2$ the average of this function from z=0 to $z=\Delta Z_{port}/2$ represents the weighting of the port area. Since $\int x(1-z^2/y^2)dz = x(z-z^3/(3y^2))$ it follows that the weighting function for the port area is the running average:

$$W_{port} = 1.4318W_{cyl}\frac{z_n - z_n^3}{3z_n(1.016^2)}$$

Where z is the normalized height of the port:

$$z_n = \frac{\Delta Z_{port}}{2\kappa a}$$

Figure 12 shows the original data from El Guebaly ("NWL p.u."), the scaled version with integral=1.0 ("NWL/avg"), the curve fit, the running average of the scaled data, and running average of the fit data.

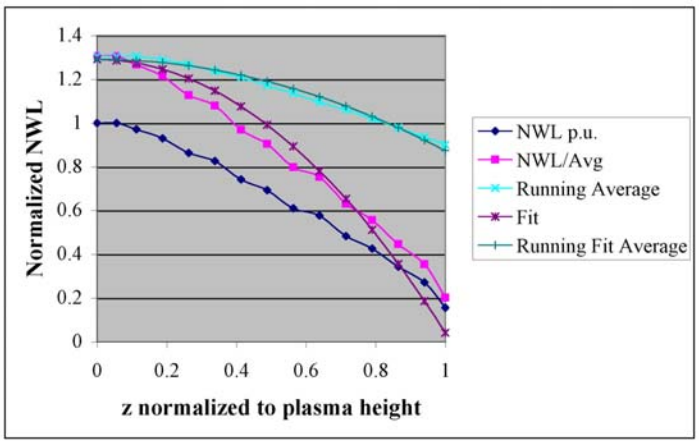

Figure 12. Outboard Neutron Flux Data

Thus the total effective area of N_{tm} test module ports, each of area $\Delta z_{port} * \Delta w_{port}$ is:

$$A_{tm\_eff} = N_{tm} W_{port} \Delta z_{port} \Delta w_{port}$$

Finally, the total available effective blanket area is the total plasma facing surface area minus the effective areas of the divertor, center stack, and ports for the NBI, RF, and Diagnostics. This assumes that all of the test module radial ports are available for blanket purposes.

$$A_{blanket} = A_{pfs} - \left[W_{cs} A_{cs} - W_{div} A_{div} - W_{port} \Delta z_{port} (2\Delta w_{port} + N_{nbi} C_{nbi}) \right]$$

Where C_{nbi} is the width of the chord corresponding to the NBI port. Then the fraction of the neutrons which reach the blanket is:

$$f_{blanket} = \frac{A_{blanket}}{A_{pfs}}$$

5.2.9 Gross Thermal Power

Electricity production is assumed derived from the power in the fusion neutrons and the radiated power to the first wall. This includes energy multiplication which takes place in the blanket due to reactions involving the neutrons and the Li isotopes. The calculation includes a toggle to select whether or not energy flow through the SOL to the divertors is recovered. Other "balance of plant" low grade heat such as dissipation in the magnets, pumping power, etc., is not recovered.

Then the total useful thermal power is:

$$P_{th} = \left[P_{neutron} f_{BEM} + (P_{\alpha} + P_{aux}) f_{rad} \right] f_{blanket} + k_{div} P_{div}$$

where:

$f_{blanket}$ = fraction of surface area covered by blanket
f_{BEM} = blanket energy multiplication factor (assumed =1.2)

5.2.10 Electric Power Consumption or Production

The calculation includes a toggle to select whether or not electricity is to be produced. If so, then with thermal to electrical energy conversion efficiency η_{EC} the gross electrical power production is:

$$P_{grosselec} = P_{th} / \eta_{EC}$$

and the operation of the "balance of plant" is assumed to consume a fraction (f_{BOP}=10%) of the gross electric power production. Otherwise the balance of plant power is assumed to be 20MW.

The conversion efficiency is typically assumed 35% for "conventional" power conversion and 45% for "advanced" power conversion" cycles.

The net electric power production is:

$$P_{netelec} = P_{grosselec} - P_{BOP} - P_{TFinput} - P_{PFinput} - P_{auxinput}$$

5.2.11 Tritium Consumption

The energy released per D-T reaction, which consumes one atom of tritium, is:

$$W = 17.586 \frac{Mev}{atom} * 1.6x10^{-19} \frac{Joule}{eV} = 2.182 \frac{Joule}{atom}$$

The mass of a tritium atom (atomic weight = 3) is:

$$M_T = \frac{3gm/mole}{6.02x10^{23}} = 4.98x10^{-24} \frac{gm}{atom}$$

Therefore the yield per unit mass is:

$$\begin{aligned} Y &= \frac{2.182J/atom}{4.98x10^{-24} gm/atom} \\ &= 5.65x10^{11} J/gm \\ &= 5.65x10^{8} MJ/kG \\ &= 6.54 MW - day/g, \end{aligned}$$

So the tritium fueling rate per day is:

$$Q_{T\_fueling} = \frac{P_{fusion}}{6.54} gm/day$$

For T breeding in the blanket, it is assumed that the blanket has a local T breeding ratio (TBR) of 1.2, i.e. 1.2 T atoms are bred from each incident neutron. So the net fractional breeding ratio (FBR) is as follows:

$$FBR = f_{blanket} TBR$$

and the net T consumption is:

$$Q_T = FBR * Q_{T\_fueling}$$

6. Solver Operations

Typically the Solver is set up to adjust the following variables to obtain a solution:

$$f_{rad}, f_{GW}, \beta_N, q_{cyl}, P_{fusion}, \eta_{CD}, J_{TF}, f_W$$

In other cases more variables may be added to this list, such as R_0 or A.

In obtaining a solution the solver iterates to satisfy the following constraints which are required for a mathematically valid solution:

1) Value of f_{rad} used to calculate τ_E, n_{He}, P_{tot} and subsequent dependent variables must be equal to ratio of calculated values P_{brem}/P_α.
2) Value of P_{fusion} used to calculate Q and subsequent dependent variables must be equal to calculated value $5*P_\alpha$.
3) Value η_{CD} must be $\leq \eta_{CDmax}$ (T) = 0.025<T>
4) Value of P_{CD} must be $\leq P_{aux}$

The following additional constraints are applied to ensure that physics and engineering limits are realistic:

1) $\beta_N \leq \beta_{Nmax}$
2) $q_{cyl} \geq q_{cylmin}$
3) $0.1 \leq f_{BS} \leq 0.99$
4) $0.1 \leq f_{GW} \leq 1$
5) $\sigma_{TF} \leq 100$MPa
6) $T_{TFCu} \leq 150$C
7) $T_{TFH20} \leq 150$C
8) $0.05 \leq f_W \leq 0.25$

Additional constraints are sometimes added to limit the solution to a particular range of interest such as:

1) HH = or $\leq$ an input value
2) N_{wall} = or $\leq$ an input value

A flow chart of solver operations is given in figure 13.

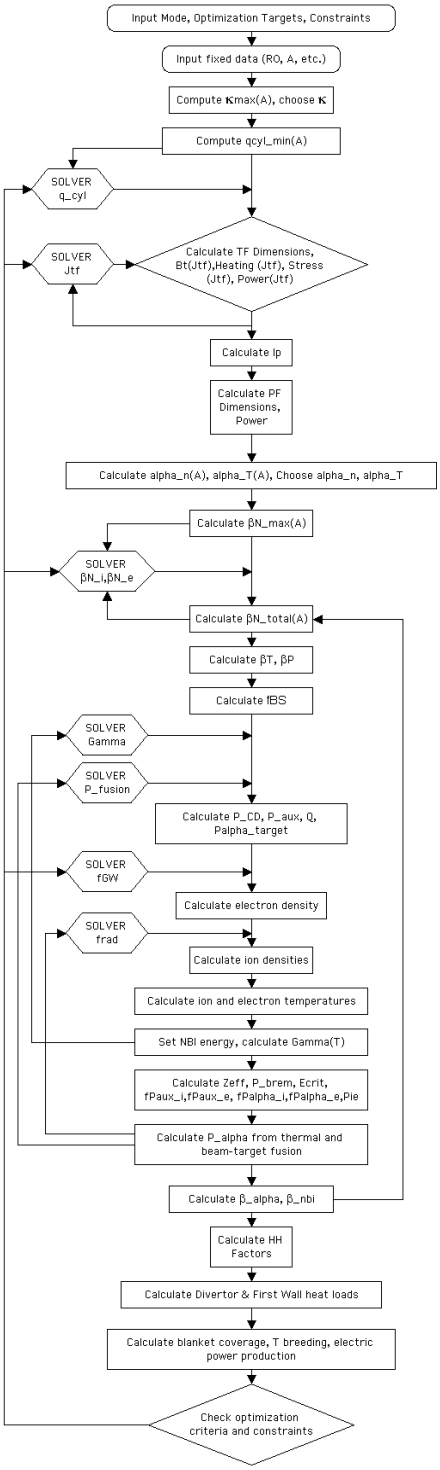

Figure 13. Solver Flow Chart

7. Sample results

Summary results from typical calculations are given in table 4 for the following cases.

NSTX:	Benchmark case
CTF:	a. 1MW/m2
	b. 4MW/m2
DEMO:	100MW net electric
REACTOR:	1GW net electric

The results listed represent the minimum major radius solutions which were found to satisfy all constraints. All cases are at A=1.5, κ=3.2 and δ=0.4. CTF cases are optimized to minimize P_aux. This is desirable in terms of minimizing cost and tritium consumption as well as maximizing available test module area.

Table 4. Sample Calculation Results

	NSTX	CTF	CTF	DEMO	REACTOR
	Benchmark	1MW/m2	4MW/m2	100MW	1000MW
R0[m]	0.880	1.200	1.200	2.200	3.100
A	1.470	1.500	1.500	1.500	1.500
kappa	2.050	3.200	3.200	3.200	3.201
delta	0.430	0.400	0.400	0.400	0.400
qMHD	9.998	11.594	7.439	7.611	7.946
qcyl	3.25	3.98	2.55	2.61	2.73
qcyl/qcyl_min	126.7%	181.2%	103.2%	100.0%	100.0%
Bt[T]	0.490	2.548	2.548	2.144	1.899
fH20		19.5%	19.5%	13.0%	12.8%
TH20max[degC]		103.7	130.3	128.7	131.0
TCumax[degC]		120.7	150.0	139.8	137.9
Sigmax[MPa]		100.0	100.0	68.3	62.5
Javgtf[A/m^2]	2.4E+07	5.3E+07	5.3E+07	2.3E+07	1.7E+07
Itf[Amp]	2.16E+06	1.53E+07	1.53E+07	2.36E+07	2.94E+07
Ip[MA]	0.800	9.602	14.964	22.562	26.989
Beta_N_thermal	3.69%	3.44%	4.78%	6.12%	6.81%
Beta_N_total	6.97%	4.11%	6.06%	7.02%	7.83%
Beta_N/Beta_N(A)	101.7%	49.8%	73.4%	85.0%	94.8%
Beta_T_alpha	0.0%	2.4%	6.8%	5.3%	6.6%
Beta_T_nbi	8.9%	0.8%	2.6%	1.2%	0.4%
Beta_T_thermal	10.1%	16.2%	35.1%	43.9%	46.8%
Beta_T_total	19.0%	19.4%	44.5%	50.4%	53.8%
Beta_P	88.0%	102.7%	91.5%	119.7%	139.1%
xne	3.0E+19	6.6E+19	1.5E+20	2.1E+20	1.5E+20
fGW	45.0%	14.5%	21.3%	65.1%	83.9%
fBS	58.0%	67.1%	59.8%	78.2%	90.0%
Tempavg[keV]	1.0	21.3	20.3	13.1	15.3
Tavgi[keV]	1.2	33.8	28.0	14.0	16.4
Tavge[keV]	0.9	10.5	13.7	12.3	14.5
HH98 (global)	1.28	2.55	1.88	1.35	1.27
HHi_NC	0.70	0.70	0.70	0.70	0.70
HHe	0.67	0.70	0.70	0.70	0.67
Tau_E_NC[sec]	0.14	20.40	19.58	24.60	35.34
Tau_E_98[sec]	0.02	0.32	0.33	0.82	1.12
Q	0.0	4.1	8.2	28.3	112.1
Zeff	1.50	1.44	1.46	1.46	1.93
P_Brem[MW]	0.0	0.5	3.3	36.0	68.9
P_rad_core[MW]	1.2	7.4	21.0	65.1	118.1
P_aux[MW]	6.0	20.7	41.1	54.3	28.2
E_nbi[keV]	90.0	104.9	240.5	604.1	615.2
P_fusion[MW]	0.0	84.3	337.1	1536.8	3156.4
P_alpha[MW]	0.0	16.9	67.4	307.4	631.3
fTC	99.8%	22.9%	15.4%	2.4%	0.5%
Gamma_CD[10^20*A/W-m^2]	0.00	0.12	0.26	0.41	0.44
P_CD[MW]	38.7	20.7	41.1	54.3	28.2
Xnwall[MW/m^2]	0.0	1.2	4.9	6.7	6.9
Qn_wall[MW/m^2]		0.64	2.55	3.45	3.57
Qn_tm[MW/m^2]		1.00	4.00	5.97	6.17
Qn_om[MW/m^2]		1.14	4.58	6.21	6.42
Port Height (delta Z)[m]		1.78	1.78	3.27	4.61
#NBI Port		1	2	1	1
Available TM Area [m]		17.8	14.3	68.7	142.9
#Test Module Ports		6	6	4	3
A_cyl_blanket[m^2]		70.2	70.2	128.8	181.5
T fueling rate[gm/day]		12.9	51.6	235.1	482.8
fCS		7.3%	7.3%	7.3%	7.3%
fN		81.6%	75.9%	85.6%	87.5%
FBR		102.0%	94.9%	107.0%	109.4%
Net T consumption rate[gm/day]		-0.25	2.62	-16.47	-45.34
n/s/W		1.0E+11	2.9E+11	1.3E+12	2.1E+12
frad_core		20.0%	20.0%	20.0%	20.0%
Q_fw[MW/m^2]		0.150	0.460	0.568	0.529
frad_div		48.7%	84.9%	83.2%	81.2%
Q_div[MW/m^2]		15.0	15.0	15.0	15.0
P_aux_input[MW]		59.2	117.4	155.1	62.6
∑P_tf[MW]		165.6	171.6	197.3	249.9
∑P_pf[MW]		0.0	0.0	0.0	0.0
P_bop[MW]		20.0	20.0	20.0	145.8
∑P_elec input[MW]		244.7	309.0	372.3	458.3
P_elec gen[MW]		0.0	0.0	472.3	1458.3
P_net elec[MW]		-244.7	-309.0	100.0	1000.0
Q_elec		0.00	0.00	1.27	3.18
Annual Elec Cost[$M]		45.0	56.9	-47.4	-474.4
Mass_TF_CS		1.6E+05	1.6E+05	6.2E+05	1.2E+06
Mass_TF_Outer		5.5E+05	5.5E+05	1.1E+06	1.7E+06
Mass_PF_Outer		5.1E+05	8.1E+05	1.7E+06	2.5E+06
P_Density[MW/m^3]		1.74	6.95	5.14	3.77

Acknowledgements

This work draws heavily on prior work by Jardin, Kessel, et al [4] as previously noted. Other important input to be noted includes that of D. Mikkelsen of PPPL on NBI physics, L. El-Guebaly on neutronics and shielding, and R.Woolley on magnet stress calculations.

References

[1] Peng Y-K M *et al* 2005 A component test facility based on the spherical tokamak *Plasma Phys. Control. Fusion* **47** B263
[2] Synakowski E *et al* 2004 *Nucl. Fusion* **43** 1648
[3] Lloyd B *et al* 2004 *Plasma Phys. Control. Fusion* **46** B477
[4] Jardin S , Kessel C, Meade D, Neumeyer C 2003 Systems analysis of a compact next step burning plasma experiment *Fusion Sci. Tech.* **43**
[5] Menard J *et al* 2003 Unified ideal stability limits for advanced tokamak and spherical torus plasmas *Princeton Plasma Physics Lab Report PPPL-3779*
[6] Wong C, Wesley J, Stambaugh R, Cheng E, 2002 Toroidal reactor designs as a function of aspect ratio and elongation *Nucl. Fusion* **42** 547
[7] Lin-Liu Y, Stambaugh R 2002 Optimum plasma states for next step tokamaks *General Atomics Report GA-A23980*
[8] Start D, Cordey J 1980 Beam induced currents in toroidal plasmas of arbitrary aspect ratio *Phys. Fluids* **23** 1477
[9] Greenwald M *et al* 1988 A new look at density limits in tokamaks *Nucl. Fusion* **28** 2199
[10] Goldston R, Rutherford P 1995 *Introduction to Plasma Physics*" (IOP Publishing, Ltd.) Chap. 14
[11] Hively L M 1977 Convenient computational forms for Maxwellian reactivities *Nucl. Fusion* **17** 873
[12] Jassby D, 1977 Neutral beam driven tokamak fusion reactors *Nucl. Fusion* **17** 309
[13] NRL Plasma Formulary 1998 Naval Research Laboratory NRL/PU/6790-98-358
[14] The ITER Team 1999 *Nucl. Fusion* **39** 2137
[15] Chang C, Hinton F 1982 *Phys. Fluids* **25** 1493
[16] Chang C, Hinton F 1986 *Phys. Fluids* **29** 3314
[17] Roark R, Young W *Formulas for Stress and Strain* (McGraw-Hill Book Co.) p. 505, formula 1f
[18] Hirshman S, Neilson G 1986 External inductance of an axisymmetric plasma *Phys. Fluids* **29** 790
[19] Voss G *et al* 1999 Spherical torus volume neutron source *Fusion Eng. Des.* **45** 257
[20] Reiersen W *et al* The TF coil design for ARIES-ST *Fusion Eng. Des.* **65** 303
[21] Cheng E *et al* 1999 Special Issue: ST VNS and Applications *Fusion Eng. Des.* **45** 257
[22] Kuriyama M *et al* 2002 Operation and development of the 500keV negative ion based neutral beam injection system for JT60-U *Fusion Sci. Tech.* **42** 410
[23] El Guebaly *et al* 2003 ARIES-ST nuclear analysis and shield design *Fusion Eng. Des.* **65** 263

External Distribution

Plasma Research Laboratory, Australian National University, Australia
Professor I.R. Jones, Flinders University, Australia
Professor João Canalle, Instituto de Fisica DEQ/IF - UERJ, Brazil
Mr. Gerson O. Ludwig, Instituto Nacional de Pesquisas, Brazil
Dr. P.H. Sakanaka, Instituto Fisica, Brazil
The Librarian, Culham Science Center, England
Mrs. S.A. Hutchinson, JET Library, England
Professor M.N. Bussac, Ecole Polytechnique, France
Librarian, Max-Planck-Institut für Plasmaphysik, Germany
Jolan Moldvai, Reports Library, Hungarian Academy of Sciences, Central Research Institute for Physics, Hungary
Dr. P. Kaw, Institute for Plasma Research, India
Ms. P.J. Pathak, Librarian, Institute for Plasma Research, India
Dr. Pandji Triadyaksa, Fakultas MIPA Universitas Diponegoro, Indonesia
Professor Sami Cuperman, Plasma Physics Group, Tel Aviv University, Israel
Ms. Clelia De Palo, Associazione EURATOM-ENEA, Italy
Dr. G. Grosso, Instituto di Fisica del Plasma, Italy
Librarian, Naka Fusion Research Establishment, JAERI, Japan
Library, Laboratory for Complex Energy Processes, Institute for Advanced Study, Kyoto University, Japan
Research Information Center, National Institute for Fusion Science, Japan
Professor Toshitaka Idehara, Director, Research Center for Development of Far-Infrared Region, Fukui University, Japan
Dr. O. Mitarai, Kyushu Tokai University, Japan
Mr. Adefila Olumide, Ilorin, Kwara State, Nigeria
Dr. Jiangang Li, Institute of Plasma Physics, Chinese Academy of Sciences, People's Republic of China
Professor Yuping Huo, School of Physical Science and Technology, People's Republic of China
Library, Academia Sinica, Institute of Plasma Physics, People's Republic of China
Librarian, Institute of Physics, Chinese Academy of Sciences, People's Republic of China
Dr. S. Mirnov, TRINITI, Troitsk, Russian Federation, Russia
Dr. V.S. Strelkov, Kurchatov Institute, Russian Federation, Russia
Kazi Firoz, UPJS, Kosice, Slovakia
Professor Peter Lukac, Katedra Fyziky Plazmy MFF UK, Mlynska dolina F-2, Komenskeho Univerzita, SK-842 15 Bratislava, Slovakia
Dr. G.S. Lee, Korea Basic Science Institute, South Korea
Dr. Rasulkhozha S. Sharafiddinov, Theoretical Physics Division, Insitute of Nuclear Physics, Uzbekistan
Institute for Plasma Research, University of Maryland, USA
Librarian, Fusion Energy Division, Oak Ridge National Laboratory, USA
Librarian, Institute of Fusion Studies, University of Texas, USA
Librarian, Magnetic Fusion Program, Lawrence Livermore National Laboratory, USA
Library, General Atomics, USA
Plasma Physics Group, Fusion Energy Research Program, University of California at San Diego, USA
Plasma Physics Library, Columbia University, USA
Alkesh Punjabi, Center for Fusion Research and Training, Hampton University, USA
Dr. W.M. Stacey, Fusion Research Center, Georgia Institute of Technology, USA
Director, Research Division, OFES, Washington, D.C. 20585-1290

The Princeton Plasma Physics Laboratory is operated
by Princeton University under contract
with the U.S. Department of Energy.

Information Services
Princeton Plasma Physics Laboratory
P.O. Box 451
Princeton, NJ 08543

Phone: 609-243-2750
Fax: 609-243-2751
e-mail: pppl_info@pppl.gov
Internet Address: http://www.pppl.gov